厚生労働科学研究費補助金

認知症対策総合研究事業

アルツハイマー病の新規細胞医薬開発に関する臨床応用研究

平成２２年度～平成２３年度　総合研究報告書

研究代表者　内村　健治

平成２４（２０１２）年　３月

別紙2

目　次

別紙３

厚生労働科学研究費補助金（認知症対策総合研究事業）
総合研究報告書

アルツハイマー病の新規細胞医薬開発に関する臨床応用研究

研究代表者　内村　健治　名古屋大学大学院医学研究科　特任准教授

研究要旨：　アルツハイマー病（AD）病態に伴って骨髄由来ミクログリア前駆細胞が脳内へ移行し、神経毒性アミロイドβタンパク（Aβ）を積極的に除去していることがADモデルマウスを用いて国内外で明らかにされた。しかしながらその脳内移行のメカニズムは未だ不明である。申請者は当該脳移行性細胞の脳内浸潤におけるセレクチン-糖鎖の分子メカニズムの重要性をADモデルマウスにより以前明らかにした。本申請研究はAD モデルマウスで得られた知見および結果をヒト臨床サンプルの使用による臨床研究へ応用するために立案された。AD 治療法開発における問題の一つは遺伝子等の効率的な脳内動員法が確立していないことである。本申請研究は脳移行性細胞を利用した細胞医薬によりこの問題を解決し、AD 新規治療法開発の技術基盤の提供を目的とする。本研究者らはヒト骨髄由来細胞株を入手しそのセレクチン認識糖鎖の発現を確認した。AD病態脳における当該細胞の動態を生体内ビデオ蛍光顕微鏡技術で解析した結果、ヒト骨髄由来細胞株のモデルマウス脳血管内におけるローリングおよび接着を観察した。一方、医療法人さわらび会福祉村病院 赤津裕康研究協力者より提供された非認知症８例、AD８例のヒト剖検脳サンプルにおけるセレクチンおよびリガンド糖鎖の発現変動を解析した。認知機能の中枢である海馬と共に提供を受けた嗅内皮質に関して発現解析を行った（計３２採取サンプル）。その結果、非認知症対照群に比べAD脳嗅内皮質でセレクチン分子の発現上昇が観察された。さらに、神経毒性重合Aβの除去を亢進させることが期待される細胞外スルファターゼ遺伝子をヒト細胞で発現し得るレンチウィルスベクターに組み込み、ウィルスを使用した遺伝子発現システムの開発に成功した。当該遺伝子を脳移行性細胞に導入しAD病態個体に投与後、脳病理変化を観察する研究への応用が期待された。ヒト臨床サンプルを用いた本申請研究は人権保護および個人情報保護に最大限の注意を払い、当該機関の倫理委員会による厳正中立な審査・承認を受けた。本研究の技術基盤により認知症を最小限に抑える研究成果が予想されその波及効果として、付随する介護負担の軽減が社会的に期待された。

Ａ．研究目的

超高齢化社会を迎えた我が国においてアルツハイマー病（AD）は増加の一途をたどっており、その治療法の確立は国民が強く求めるものとなっている。ADは神経毒性を引き起こす重合アミロイドβタンパク（Aβ）の沈着が脳内で生成され、神経細胞死やシナプスの機能障害・脱落が生じることにより認知症が発症すると主に考えられている。本研究は脳移行性細胞を重合 Aβ分解／阻止分子の脳内搬送体として利用し、AD治療における細胞医薬技術基盤の確立を目指す。骨髄由来ミクログリアがAD病態に伴い脳内に浸潤することがモデルマウスを用いた解析により報告された（Simard et al., Neuron, 2006; El Khoury et al., Nat Med 2007など）。脳内へ移行した骨髄由来ミクログリア細胞は神経毒性 Aβを積極的に除去していることが国内外で明らかにされた。しかしながらその脳内移行のメカニズムは不明である。申請者は以前、末梢投与

マウスミクログリア細胞の脳内動態を生体内ビデオ蛍光顕微鏡によりイメージング解析することに成功した。すなわち、当該脳移行性細胞の脳内浸潤におけるセレクチン-糖鎖の分子メカニズムの重要性をADモデルマウスにより明らかにした。本申請研究はADモデルマウスで得られた知見および結果をヒト臨床サンプルの使用による臨床研究へ応用するために立案された。AD 治療法開発における問題の一つは遺伝子等の効率的な脳内動員法が確立していないことである。本申請研究は脳移行性細胞を利用した細胞医薬によりこの問題を解決し、AD 新規治療法開発の技術基盤を提供することを目的とする。

B．研究方法

本研究は研究代表者である申請者が研究総括、実験計画の立案および遂行を行った。リサーチレジデント１名は生体内ビデオ蛍光顕微鏡を用いた脳内細胞イメージング解析および組織染色を研究協力した。医療法人さわらび会福祉村病院 長寿医学研究所 赤津裕康副所長よりヒト剖検脳の試料提供と研究協力を受けた。申請者は生体内ビデオ蛍光顕微鏡を本研究室に設置し末梢投与マウス骨髄由来ミクログリア細胞のADモデルマウス脳内におけるローリングおよび接着のイメージング解析に成功した。この成果をヒト骨髄由来細胞へ応用した。ヒト骨髄由来細胞は市販のヒト細胞株 U937 を用いた。ADモデルマウスは加齢育成したTg2576またはJ20 マウスを使用した。アルツハイマー病および非認知症対照群でそれぞれ８例の剖検脳凍結サンプル（海馬および嗅内皮質）の提供を受けた。セレクチンおよびリガンド糖鎖の発現をウェスタンブロット法により解析した。我々のADモデルマウスの結果ではE-セレクチンの発現誘導が観察されているのでヒト剖検脳においてもE-セレクチンを重点的に検証した。また、セレクチンが認識するシアリルルイス X 様糖鎖リガンドの発現も同様に解析した。(医療法人さわらび会福祉村病院で死亡し病理解剖を行った症例の中で、採取サンプルの研究目的の使用に承諾が得られた剖検試料を解析した。）ヒト剖検脳サンプルは以下の方法で調整した。１）凍結脳サンプルを Tris-buffered saline (TBS)に懸濁し超音波処理した。遠心後の上清を TBS 可溶画分として回収した。２）遠心後の沈殿物を 1%SDS に懸濁し超音波処理した。遠心後の上清を SDS 可溶画分として回収した。３）遠心後の沈殿物を 98%ギ酸に懸濁しギ酸可溶画分として回収した。骨髄由来ミクログリア前駆細胞に細胞外スルファターゼSulf遺伝子をウィルスベクターの使用により導入し、AD モデルマウスに移植する試験の技術開発を行った。実験解析の実施はすべて本研究者の所属機関とし、徹底した当該機関の倫理審査の承認のもとで行った。医療法人さわらび会福祉村病院で死亡し病理解剖を行った症例の中で、採取サンプルの研究目的の使用に承諾が得られた剖検試料を解析した。

（倫理面への配慮）

研究実施に先立ち、各研究実施協力機関の倫理委員会による厳正中立な審査を受け、研究実施計画の承認を受ける。特にヒト試料を用いた研究実施に際しては人権の保護および個人情報の保護に最大限の注意を払うことを理解遵守し一層の徹底を図る。また、１）インフォームドコンセントの徹底、２）検体の使用及び保存についての中止請求を含む研究協力同意書の十分な説明、３）検体保存責任者を設置し当該者以外には連結不可能な匿名化を施したうえでのサンプル及びデータの保管、さらにスタンドアローンのコンピューターを用いたデータ処理、鍵のかかるキャビネット内へのデータ保管を行う。 本研究において遺伝子の抽出・保管および遺伝子発現の解析は行わず、遺伝情報に触れる事はない。

研究実施に先立ち、研究実施機関の倫理委員会による厳正中立な審査を受け、研究実施計画の承認を受けた。本申請研究

で実施するモデルマウス対象研究はすべて当該機関設置の遺伝子組換え生物実験安全委員会の審査を受け承認を得た。また、当該機関設置の実験動物委員会および動物実験倫理委員会の審査を受け承認を得た。本研究課題に参画する者は「遺伝子組換え生物等の使用等の規制による生物の多様性の確保に関する法律（カルタヘナ法)」、「動物の愛護及び管理に関する法律」および「動物を用いる生物医学研究のための国際指導原則」の更なる理解を確認し遵守した。

C．研究結果

ヒト骨髄由来細胞株がモデルマウス脳血管内でローリングおよび接着を示す結果を得た。また、当該細胞でセレクチンリガンド糖鎖の発現が観察された。AD 嗅内皮質および海馬におけるセレクチンリガンド糖鎖の発現を検証したが困難であったため、リガンド糖鎖合成酵素の発現を検証した。AD 群においてセレクチンリガンド糖鎖合成酵素の一種が特異的に発現上昇を示した。リガンド糖鎖およびその合成酵素の AD 群における特異的発現上昇を確認した。神経毒性重合 Aβの除去を亢進させることが期待される細胞外スルファターゼ遺伝子をレンチウィルスベクターに組み込み、ヒト細胞で発現し得る遺伝子発現システムの開発に成功した。

D．考察

AD 剖検脳におけるセレクチンリガンド糖鎖合成酵素の特異的発現上昇は AD モデルマウスで観察された骨髄由来ミクログリア細胞が AD 病態に伴って脳内へ移行するという現象がヒトでも起きている可能性をさらに強く示唆した。神経毒性重合 Aβの除去を亢進させることが強く期待される細胞外スルファターゼ遺伝子を脳移行性細胞に恒常的に発現させ、血行性にアルツハイマー病態脳内へ送り込む細胞医薬開発の技術基盤を確立した。

E．結論

アルツハイマー病の病態に伴う骨髄由来ミクログリア細胞の脳内移行がヒト AD 脳でも起きている可能性が示された。確立した遺伝子発現システムを使用し、今後アルツハイマー病細胞医薬開発に貢献することが強く期待された。

F. 健康危険情報

該当なし。

G．研究発表

１．論文発表

Hossain MM, Hosono-Fukao T, Tang R, Hosono-Fukao, T., Ohtake-Niimi, S., Nishitsuji, K., Hossain, M. M., van Kuppevelt, T. H., Michikawa, M. and Uchimura, K. RB4CD12 epitope expression and heparan sulfate disaccharide composition in brain vasculature.
J. Neurosci. Res., 89:1840-1848 (2011)

Nishitsuji, K., Hosono, T., Uchimura, K. and Michikawa, M. Lipoprotein lipase is a novel Abeta- binding protein that promotes glycosaminoglycan-dependent cellular uptake of Abeta in astrocytes.
J. Biol. Chem., 286:6393-6401 (2011)

内村健治
細胞外スルファターゼ Sulf によるヘパラン硫酸糖鎖機能の調節　生化学　83: 216-223, (2011)

Hosono-Fukao, T., Ohtake-Niimi, S., Hoshino, H., Britschgi, M., Akatsu, H., Hossain, M. M., Nishitsuji, K., van Kuppevelt, T. H., Kimata, K., Michikawa, M. Wyss-Coray, T. and Uchimura, K. Heparan sulfate subdomains that are degraded by Sulf accumulate in cerebral amyloid beta plaques of Alzheimer's disease: Evidence from mouse models and patients.
Am. J. Pathol., 180:2056-2067 (2012)

Fujiwara M, Kobayashi M, Hoshino H, Uchimura K, Nakada T, Masumoto J, Sakai Y, Fukuda M, Nakayama J. Expression of Long-form
N-Acetylglucosamine-6-O-Sulfotransferase 1

in Human High Endothelial Venules.
J. Histochem. Cytochem. 60:397-407 (2012)

２．学会発表

Hosono T, Hossain M, Britschgi M, Akatsu H,van Kuppevelt T, Michikawa M, Wyss-Coray T, Uchimura K.
The Sulf-degrading heparan sulfate epitope accumulates in cerebral amyloid ß plaques of mouse models and patients of Alzheimer's disease
25th International Carbohydrate Symposium (ICS2010) Makuhari Messe, Makuhari, Aug, 2, 2010

Hossain M, Hosono T, Niimi S, van Kuppevelt T, Michikawa M, Rosen S, Uchimura K.
Immunolocalization of the RB4CD12 anti-heparan sulfate epitope in the brain and its degradation by Sulfs, extracellular endosulfatases
25th International Carbohydrate Symposium (ICS2010) Makuhari Messe, Makuhari, Aug, 5, 2010

内村健治
セレクチン認識および血管外細胞遊走に関わる糖鎖関連酵素
-骨髄由来細胞のアルツハイマー病脳内浸潤-
第４回ミッドカイン研究会　名古屋大学医学部　2010 年 8 月 9 日、名古屋

内村健治
アルツハイマー病モデルマウス脳内に発現されるケラタン硫酸糖鎖の解析
第１回加藤記念バイオサイエンス研究振興財団研究発表会 2010 年 10 月 22 日、東京

細野友美、新美しおり、モタラブホサイン、マーカスブリッチギ、赤津裕康、菅谷典子、木全弘治, 道川誠、トニーワイスコレイ, 内村健治
アルツハイマー病モデルマウス脳内に発現するヘパラン硫酸糖鎖の内部ドメイン構造の解析　第 29 回日本認知症学会 2010 年 11 月 5 日、名古屋

Fukao-Hosono T, Hossain M, Ohtake-Niimi S , van Kuppevelt T , Michikawa M, Rosen S and Uchimura K　Immunolocalization of the RB4CD12 Anti-Heparan Sulfate Epitope in Brain Microvessels and Its Degradation by Sulf-1 and Sulf-2　Annual meeting of Glycobiology 2010, St. Pete Beach, USA, Nov 8, 2010

細野友美、新美しおり、ホサインモタラブ、菅谷典子、赤津裕康、トニーワイスコレイ、木全弘治、道川誠、内村健治
アルツハイマー病モデルマウス大脳皮質に発現するヘパラン硫酸グリコサミノグリカンの構造解析　第 83 回日本生化学会大会　2010 年 12 月 9 日、神戸

Kenji Uchimura
Selectin-carbohydrates interaction in extravasation of bone marrow-derived cells into Alzheimer brain
Wyss-Coray Lab Seminar, Stanford University, 2/14/2011, Palo Alto

内村健治
細胞の血行性組織内浸潤に関わる細胞表面セレクチンとそのリガンド糖鎖
リンパ球ホーミング，骨髄細胞アルツハイマー病脳内浸潤
信州大学大学院医学研究科、2011 年 5 月 30 日、松本

新美しおり，星野瞳，道川誠，門松健治，内村健治
アルツハイマー病モデルマウス脳に発現するコンドロイチン硫酸グリコサミノグリカンの構造解析
第 84 回日本生化学会大会　2011 年 9 月 23 日、京都

星野瞳，新美しおり，道川誠，神奈木玲児，内村健治
セレクチンリガンド形成に関わる硫酸転移酵素は生後マウス発達脳における 5D4 ケラタン硫酸糖鎖抗原の発現を制御する
第 84 回日本生化学会大会　2011 年 9 月 23 日、京都

新美しおり，星野瞳，細野友美，道川誠，内村健治
アルツハイマー病モデルマウス脳に発現する細胞外マトリックスコンドロイチン硫酸糖鎖の構造解析
第 30 回日本認知症学会　2011 年 11 月 12 日、東京

Hitomi Hoshino, Shiori Ohtake-Niimi, Makoto Michikawa, Reiji Kannagi, and Kenji Uchimura
Sulfotransferases that regulate expression of the 5D4 keratan sulfate epitope in early postnatal mouse brain
Annual meeting of Glycobiology 2011, Seattle, USA, Nov 11, 2011

H. 知的財産権の出願・登録状況（予定を含む。）
１．特許取得
なし

２．実用新案登録
なし

３．その他
なし

別紙４

研究成果の刊行に関する一覧表

雑誌

発表者氏名	論文タイトル名	発表誌名	巻号	ページ	出版年
Hosono-Fukao, T., Ohtake-Niimi, S., Nishitsuji, K., Hossain, M. M., van Kuppevelt, T. H., Michikawa, M. and Uchimura, K.	RB4CD12 epitope expression and heparan sulfate disaccharide composition in brain vasculature.	***J. Neurosci. Res.***	89	1840-48	2011
Nishitsuji, K., Hosono, T., Uchimura, K. and Michikawa, M	Lipoprotein lipase is a novel Abeta- binding protein that promotes glycosaminoglycan-dependent cellular uptake of Abeta in astrocytes.	***J. Biol. Chem.***	286	6393-6401	2011
内村健治	細胞外スルファターゼ Sulf によるヘパラン硫酸糖鎖機能の調節	生化学	86	216-223	2011
Hosono-Fukao, T., Ohtake-Niimi, S., Hoshino, H., Britschgi, M., Akatsu, H., Hossain, M. M., Nishitsuji, K., van Kuppevelt, T. H., Kimata, K., Michikawa, M. Wyss-Coray, T. and Uchimura, K.	Heparan sulfate subdomains that are degraded by Sulf accumulate in cerebral amyloid beta plaques of Alzheimer's disease: Evidence from mouse models and patients.	***Am. J. Pathol.,***	180	2056-2067	2012
Fujiwara M, Kobayashi M, Hoshino H, Uchimura K, Nakada T, Masumoto J, Sakai Y, Fukuda M, Nakayama J.	Long-form N-Acetylglucosamine-6-O-Sulfotransferase 1 in Human High Endothelial Venules.	***J. Histochem. Cytochem.***	60	397-407	2012

研究成果の刊行物・別刷

Journal of Neuroscience Research

Journal of Neuroscience Research 89:1840–1848 (2011)

RB4CD12 Epitope Expression and Heparan Sulfate Disaccharide Composition in Brain Vasculature

Tomomi Hosono-Fukao,[1] Shiori Ohtake-Niimi,[1] Kazuchika Nishitsuji,[2] Md. Motarab Hossain,[1] Toin H. van Kuppevelt,[3] Makoto Michikawa,[2] and Kenji Uchimura[1,2]*

[1]Section of Pathophysiology and Neurobiology, National Center for Geriatrics and Gerontology, Aichi, Japan
[2]Department of Alzheimer's Disease Research, National Center for Geriatrics and Gerontology, Aichi, Japan
[3]Department of Biochemistry 280, Nijmegen Centre for Molecular Life Sciences, Radboud University Nijmegen Medical Center, Nijmegen, The Netherlands

RB4CD12 is a phage display antibody that recognizes a heparan sulfate (HS) glycosaminoglycan epitope. The epitope structure is proposed to contain a trisulfated disaccharide, [–IdoA(2-OSO_3)-$GlcNSO_3$(6-OSO_3)–], which supports HS binding to various macromolecules such as growth factors and cytokines in central nervous tissues. Chemically modified heparins that lack the trisulfated disaccharides failed to inhibit the RB4CD12 recognition of HS chains. To determine the localization of the RB4CD12 anti-HS epitope in the brain, we performed an immunohistochemical analysis for cryocut sections of mouse brain. The RB4CD12 staining signals were colocalized with laminin and were detected abundantly in the vascular basement membrane. Bacterial heparinases eliminated the RB4CD12 staining signals. The RB4CD12 epitope localization was confirmed by immunoelectron microscopy. Western blotting analysis revealed that the size of a major RB4CD12-positive molecule is ~460 kDa in a vessel-enriched fraction of the mouse brain. Disaccharide analysis with reversed-phase ion-pair HPLC showed that [–IdoA(2-OSO_3)-$GlcNSO_3$(6-OSO_3)–] trisulfated disaccharide residues are present in HS purified from the vessel-enriched brain fraction. These results indicated that the RB4CD12 anti-HS epitope exists in large quantities in the brain vascular basement membrane.

Key words: basement membrane; brain vessels; heparan sulfate; HPLC; scFv antibody

Heparan sulfate proteoglycans (HSPGs) are found on the cell surface and in the extracellular matrix, and they consist of core protein to which one or more heparan sulfate (HS) chains are covalently bound (Bernfield et al., 1999; Esko and Lindahl, 2001). HS chains and heparins, structural analogues of HS chains, are members of the family of glycosaminoglycans made up of repeating disaccharide units of glucuronic/iduronic acid (GlcA/IdoA) and glucosamine (GlcN), which are modified through a set of deacetylation, epimerization, and sulfation reactions (Gallagher, 2001). The *N*-, 3-*O*, and 6-*O* positions of GlcN and the 2-*O* position of the uronic acid residues in the disaccharide units are potentially substituted by sulfate groups by a series of Golgi-resident HS sulfotransferases (Habuchi et al., 2004). These synthetic reactions along the HS chains are spatially and temporally regulated, conferring upon the chains structural diversity, which underlies important roles in pathological and biological processes (Nakato and Kimata, 2002; Parish, 2006; Bishop et al., 2007; Yan and Lin, 2009). HS contains highly sulfated domains and partially sulfated or nonsulfated domains, which are transitional (Gallagher, 2001). Highly sulfated domains are the most common units in heparin. Within the domains, a trisulfated disaccharide structure [–IdoA(2-OSO_3)-$GlcNSO_3$(6-OSO_3)–] is present. This structure is considered to be a key element in molecular interactions between HS/heparin and many ligands, including growth factors, chemokines, morphogens, and lipopro-

Contract grant sponsor: Japanese Health and Labour Sciences Research Grants (Comprehensive Research on Aging and Health); Contract grant number: H19-001; Contract grant number: H22-007 (to K.U.); Contract grant sponsor: Ministry of Education, Science, Sports, Culture; Contract grant number: 22790303 (to K.U.); Contract grant sponsor: Takeda Science Foundation (to K.U.); Contract grant sponsor: Kato Memorial Bioscience Foundation (to K.U.); Contract grant sponsor: Uehara Memorial Foundation (to K.U.).

*Correspondence to: Kenji Uchimura, Section of Pathophysiology and Neurobiology, Department of Alzheimer's Disease Research, National Center for Geriatrics and Gerontology, 35 Gengo, Morioka, Obu, Aichi 474-8511, Japan. E-mail: arumihcu@ncgg.go.jp

Received 6 February 2011; Revised 9 April 2011; Accepted 11 April 2011

Published online 29 July 2011 in Wiley Online Library (wileyonlinelibrary.com). DOI: 10.1002/jnr.22690

teins (Bernfield et al., 1999; Esko and Selleck, 2002). The trisulfated disaccharides of heparin (Morimoto-Tomita et al., 2005; Saad et al., 2005) and heparan sulfate (Ai et al., 2003; Viviano et al., 2004; Lamanna et al., 2008) are degraded by endoglucosamine 6-sulfatases, Sulf-1 and Sulf-2, in the extracellular space. The Sulfs are thought to reverse the association between angiogenic factors and heparin/HSPGs (Morimoto-Tomita et al., 2005; Uchimura et al., 2006).

Vessels in the brain are essential for functions of the blood–brain barrier as well as CNS angiogenesis (Risau and Wolburg, 1990). The brain vasculature is also considered to be a niche that conditions brainstem cells for further lineaging (Palmer et al., 2000). Molecules of the basement membrane of brain vasculature include HSPGs and laminin. The basement membrane HSPGs can function as both pro- and antisignaling molecules. They can stimulate cell signaling by binding to and concentrating growth factors through their HS chains in close proximity to cell-surface receptors. On the other hand, basement membrane HSPGs can reduce signaling by sequestering growth factors away from their receptors. Regulation is achieved by the balance of inhibitory vs. stimulatory forms of HS, which is ultimately controlled by the specific sulfation modifications on the HS chains (Gallagher, 2001).

To evaluate the expression and localization of the specific sulfation modifications of HS in cultures and tissues, antibodies against HS have been established as useful tools (van den Born et al., 2005). The HS epitopes of recently developed phage display antibodies have been defined using derivatives of HS and heparins (van Kuppevelt et al., 1998). One of them, RB4CD12, recognizes *N*- and *O*-sulfated saccharides of HS/heparin (Dennissen et al., 2002; Jenniskens et al., 2000). The *N*-, 2-*O*, and 6-*O* sulfation and C-5 epimerization of HS are important determinants for the antibody recognition. The recognition epitope is proposed to be a trisulfated disaccharide-containing HS oligosaccharide (Jenniskens et al., 2002). We have shown that the RB4CD12 epitope is degraded by Sulfs in vitro and ex vivo and that the antibody can be utilized to measure the activity of the Sulfs (Hossain et al., 2010; Lemjabbar-Alaoui et al., 2010; Uchimura et al., 2010). Here we describe the RB4CD12 anti-HS epitope abundant in the brain vascular basement membrane and structural analysis of HS chains in brain vessel-enriched fractions.

MATERIALS AND METHODS

Materials

The RB4CD12 phage display-derived antiheparan sulfate antibody (also known as HS3A8) was produced as a VSV (vesicular stomatitis virus)-tag version and purified as described previously (Dennissen et al., 2002). The following materials were obtained commercially from the sources indicated. Heparin conjugated with bovine serum albumin (heparin-BSA), heparinases (I, II, and III), polyclonal rabbit antilaminin antibody (Ab), monoclonal anti-VSV glycoprotein-Cy3 Ab, monoclonal anti-FLAG Ab, and biotinylated WFA lectin were from Sigma (St. Louis, MO); *N*-desulfated, 2-*O*-desulfated, and 6-*O*-desulfated heparins were from Neoparin (Alameda, CA); polyclonal rabbit anti-VSV-G Ab was from Bethyl Laboratories (Montgomery, TX); alkaline phosphatase-conjugated polyclonal goat anti-rabbit IgG (H + L), Cy2-conjugated goat anti-mouse IgG (H + L), and Cy2-conjugated goat anti-rabbit IgG (H + L) were from Jackson Immunoresearch Laboratories (West Grove, PA); biotinylated swine anti-goat IgG (H + L) and streptavidin conjugated with alkaline phosphatase were from Caltag Laboratories (Burlingame, CA); mouse anti-NeuN Ab was from Millipore (Billerica, MA); rabbit anti-Iba1 Ab was from Wako Pure Chemical Industries (Osaka, Japan); rabbit anti-GFAP Ab was from Thermo Scientific (Rockford, IL); mouse anti-CNPase Ab was from Abcam (Cambridge, MA); chondroitinase ABC, keratanase I, hyaluronidase, chondroitin, and chondroitin sulfate C were from Seikagaku (Tokyo, Japan); polyclonal goat anti-rabbit IgG Nanogold, diameter 1.4 nm was from Nanoprobes (Yaphank, NY); and horseradish peroxidase-conjugated goat anti-rabbit IgG was from Cell Signaling Technology (Beverly, MA).

Animals

C57BL/6 mice were from Japan SLC Inc. (Hamamatsu, Japan). Mice were maintained in barrier facilities. The National Center of Geriatrics and Gerontology Institutional Animal Care and Use Committee approved the animal studies.

ELISA for RB4CD12 Recognition

To immobilize heparin, 100 ng/ml heparin-BSA in PBS was added to the wells (100 μl/well) of a 96-well plate (Immulon 2HB; Dynex Laboratories). The plate was kept at 4°C overnight. The wells were washed three times with PBS containing 0.1% Tween-20 (PBS-T) and then blocked with 3% BSA (Sigma) in PBS containing 0.01% NaN_3 at room temperature (RT) for 2 hr. The wells were washed as descfribed above and incubated with 100 μl/well RB4CD12 (1:750 diluted by 0.1% BSA in PBS) mixed with intact heparins, chemically modified heparins, chondroitin sulfates, or heparinase-treated heparins at RT for 1 hr. The wells were washed as described above and incubated with 100 μl/well secondary rabbit anti-VSV antibody (1 μg/ml in 0.1% BSA in PBS) at RT for 45 min. Then, the wells were washed and incubated with 100 μl/well of alkaline phosphatase-conjugated goat anti-rabbit IgG (0.3 μg/ml in 0.1% BSA in PBS) at RT for 45 min. The wells were washed as described above and incubated with p-nitrophenyl phosphate (PNPP; Pierce, Rockford, IL) at RT for 5 to 10 min. OD 405 nm was read on a microplate reader (Bio-Rad, Hercules, CA).

Fractionation of Brain Samples

A snap-frozen mouse cortex (~25 mg) was placed in a tube containing 600 μl (30 vol of the tissue weight) of ice-cold TBS (20 mM Tris and 137 mM NaCl, pH 7.6) and protease inhibitors (complete protease inhibitor cocktail; Roche Diagnostics, Indianapolis, IN). The tube was placed in a water bath of the Bioruptor ultrasonic vibration (CosmoBio, Tokyo, Japan). The tissue was fragmented by sonicating the tube for

15 sec with the maximum ultrasonic wave output power four or five times until solid materials in the tube became invisible. The material was ultracentrifuged at 100,000*g* for 20 min at 4°C. The supernatant was collected and stored frozen as the "TBS-soluble fraction." The resulting precipitate was suspended in 600 μl (the same volume as mentioned above) of TBS containing 1% SDS. The suspension was centrifuged at 12,000 rpm for 20 min at RT. The resulting supernatant was collected and stored frozen as the "SDS-soluble fraction." The protein concentrations of both fractions were measured with a BCA Protein Assay Reagent Kit (Thermo Scientific). Twenty-five milligrams of frozen mouse brain cortex was placed on a glass Petri dish and minced with a blade. The tissues were transferred into a tube containing 1 ml ice-cold TBS. The tissues were homogenized with a Dounce homogenizer. The homogenate was filtered with a 100-μm nylon mesh. The filtered materials were collected and then applied to a 40-μm nylon mesh. Residues on the filters were suspended in 100 μl TBS containing 1% SDS ("vessel-enriched fraction"). Materials filtered through the 40-μm nylon mesh were collected and mixed with the same volume of TBS containing 2% SDS ("flow-through fraction"). Methylene blue staining and brightfield microscopy confirmed cerebral blood vessels on the filters.

Immunohistochemistry

Fresh brains from 12-week-old C57BL/6 mice were embedded in the O.C.T. compound (Sakura Finetek, Torrance, CA) and frozen in liquid nitrogen. The brains were stored at −80°C until analysis. Cryostat-cut sections (10 μm thick) were prepared on MAS-coated glass slides (Matsunami, Osaka, Japan), fixed in ice-cold acetone for 15 min, and then air dried for 30 min. Sections were incubated with blocking solution (3% BSA in PBS) for 15 min at RT. Sections were washed twice with PBS and then incubated with a mixture of RB4CD12 (1:100 dilution) and rabbit antilaminin antibody (1:100 dilution; Sigma) for 1 hr at RT. Then, primary antibodies were detected with Cy3-conjugated monoclonal anti-VSV-G (4 μg/ml) and Cy2-conjugated polyclonal goat anti-rabbit IgG (3 μg/ml). Sections were mounted in FluorSave Reagent (Merck, Darmstadt, Germany). Digital images were captured by fluorescent microscopy (model BX50; Olympus) at the same setting for all images. To determine the effects of GAG-degrading enzymes, 3% BSA-blocked sections were pretreated with 100 μl of a reaction mixture containing 5 μmol HEPES, pH 7.5, and enzymes (a mixture of 1 mU heparinase I, 0.25 mU heparinase II, 0.1 mU heparinase III, 50 mU chondroitinase ABC, 250 mU keratanase I, or 250 mTRU hyaluronidase) at 37°C overnight. For pretreatment with the mixture of heparitinases, 1 μmol $MgCl_2$ was added to the reaction mixture.

Immunoelectron Microscopy

Cryostat-cut sections from 12-week-old C57BL/6 mouse brain were prepared on MAS-coated glass slides, fixed in 4% paraformaldehyde for 5 min, then washed with PBS for 1 hr. Sections were incubated with 3% BSA for 30 min at RT. Diluted RB4CD12 antibody (1:40) was then applied overnight. After washing, diluted rabbit anti-VSV secondary (7.2 μg/ml) was applied for 1 hr. After several washes, diluted goat anti-rabbit IgG antibody coupled with 1.4-nm-diameter tertiary gold particles (1:40) was applied for 30 min. The samples were then washed and fixed in 2% glutaraldehyde in 0.1 M sodium cacodylate buffer (pH 7.4) for 3 hr, followed by enlargement of the gold particles with an HQ-Silver Enhancement Kit (Nanoprobes). The specimens were examined in a Hitachi H-7600 transmission electron microscope.

Immunoblots

The proteins (40 μg per lane) were separated by NuPAGE 3–8% polyacrylamide gel electrophoresis (Invitrogen, Carlsbad, CA) and blotted onto a PVDF membrane (Millipore, Bedford, MA). The membrane was blocked with 5% skim milk /PBS-T for 1 hr at room temperature and then incubated overnight with RB4CD12 antibody (1:500) in TBS-T at 4°C. The membrane was washed and incubated with horseradish peroxidase-conjugated mouse anti-VSV (1:2,000) for 1 hr at RT. Bound antibodies were visualized with SuperSignal West Dura Chemiluminescent reagent (Thermo Scientific). Signals were visualized and quantified using a LAS-3000 mini-luminescent image analyzer (Fujifilm, Tokyo, Japan).

Preparation and Structural Analysis of HS

Two hundred fifty milligraqms of frozen mouse cortex or the cortical vessel residue that remained on the filters described above was suspended in 2 ml of 0.2N NaOH and incubated overnight at RT. The samples were neutralized with 4 N HCl and then treated with DNase I and RNase A (0.04 mg/ml each; Roche) in 50 mM Tris-HCl, pH 8.0, 10 mM $MgCl_2$ for 3 hr at 37°C. Subsequently, the samples were treated with actinase E (0.04 mg/ml; Kaken Pharmaceutical, Tokyo, Japan) overnight at 37°C. The supernatant was collected by centrifugation at 5,000*g* at 4°C for 10 min after heat inactivation of the enzyme and then mixed with the same volume of 50 mM Tris-HCl, pH 7.2. The HS was purified by DEAE-Sepharose column chromatography as reported previously (Habuchi et al., 2007). The disaccharide compositions of the HS were determined by reversed-phase ion-pair chromatography with postcolumn fluorescent labeling adapted from a method described in a previous report (Toyoda et al., 2000). The level of total HS was determined by summing amounts of all disaccharides detected in each sample. All data are presented as mean ± SD unless noted otherwise. The values were analyzed in Prism software (GraphPad Software, La Jolla, CA).

RESULTS

Modified Heparins That Lack Trisulfated Disaccharide Units Do Not Interfere With the RB4CD12 Recognition

RB4CD12 is a single-chain variable-fragment (scFv) antibody selected for reactivity to skeletal muscle heparin/HS glycosaminoglycans utilizing a phage display system (Jenniskens et al., 2000). Antibody binding depends on all three sulfate modifications (Dennissen et al., 2002). To characterize further the RB4CD12

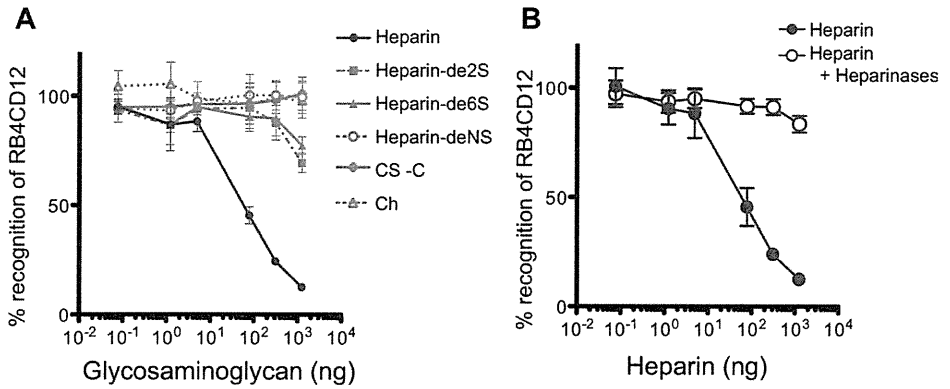

Fig. 1. Inhibition ELISA for the RB4CD12 recognition determinant. **A:** Binding of the RB4CD12 antibody to heparin-BSA-coated on plates was measured in the presence of heparin, chemically modified heparin, or chondroitin sulfate shown at right. **B:** The binding of RB4CD12 in the presence of heparin that was pretreated with a mixture of heparinase I, heparinase II, and heparinase III was measured. Hep-de2S, 2-*O*-desulfated heparin; Hep-de6S, 6-*O*-desulfated heparin; Hep-deNS, *N*-desulfated heparin; CS-C, chondroitin 6-sulfate; Ch, chondroitin.

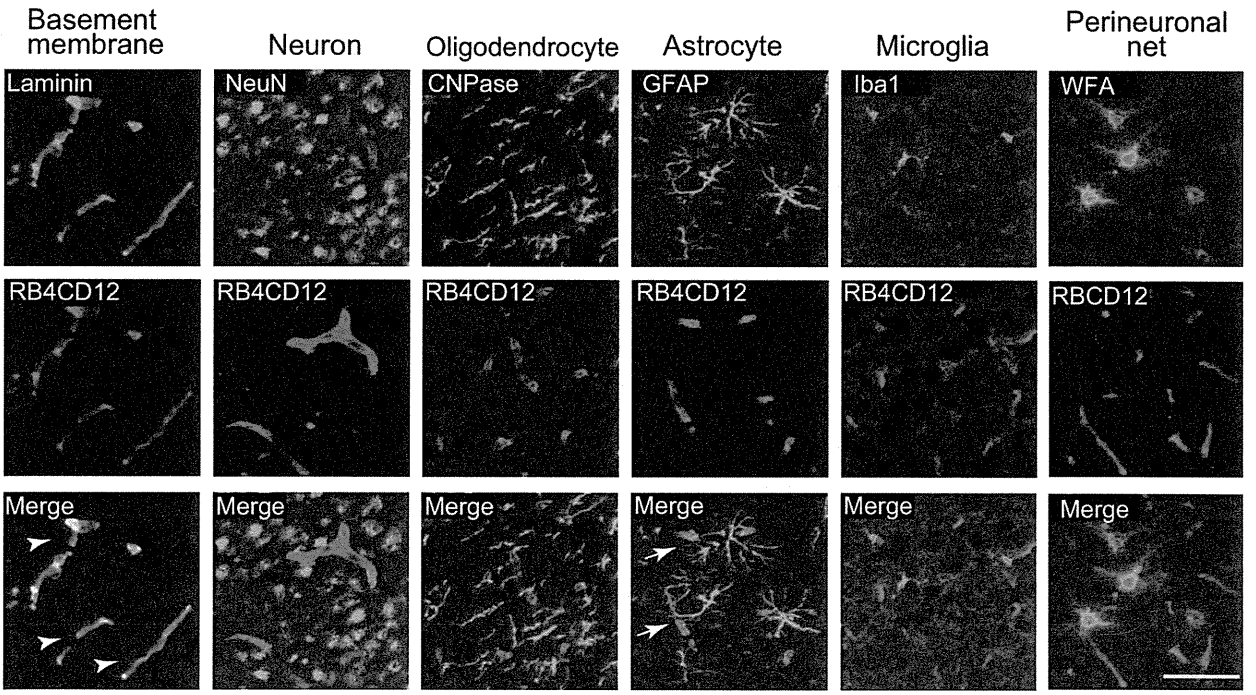

Fig. 2. Immunoreactivity of RB4CD12 is colocalized with laminin in the mouse brain. RB4CD12 binding was visualized using a Cy3-conjugated anti-VSV tag antibody with fluorescence microscopy (red). Basement membrane of brain vasculature and different types of cells were costained by cell-type-specific antibodies, laminin, NeuN, CNPase, GFAP, Iba1, or biotinylated WFA lectin in conjunction with Cy2-conjugated secondary antibodies or streptavidin (green). RB4CD12 staining signals were colocalized with laminin staining in the basement membrane of brain vessels (arrowheads). GFAP partially colocalized with the RB4CD12 signals at the interface between vessels and astrocytes (arrows). Scale bar = 50 μm.

recognition determinants, we performed a cell-free ELISA with chemically modified heparins. The RB4CD12 antibody recognized heparin-BSA (10 ng) immobilized onto plastic wells (Fig. 1). RB4CD12 binding to heparin-BSA was substantially reduced by premixing with an intact heparin in a dose-dependent manner. Chemically modified heparins that are 2-*O*-desulfated or 6-*O*-desulfated showed much less inhibition even at higher concentra-

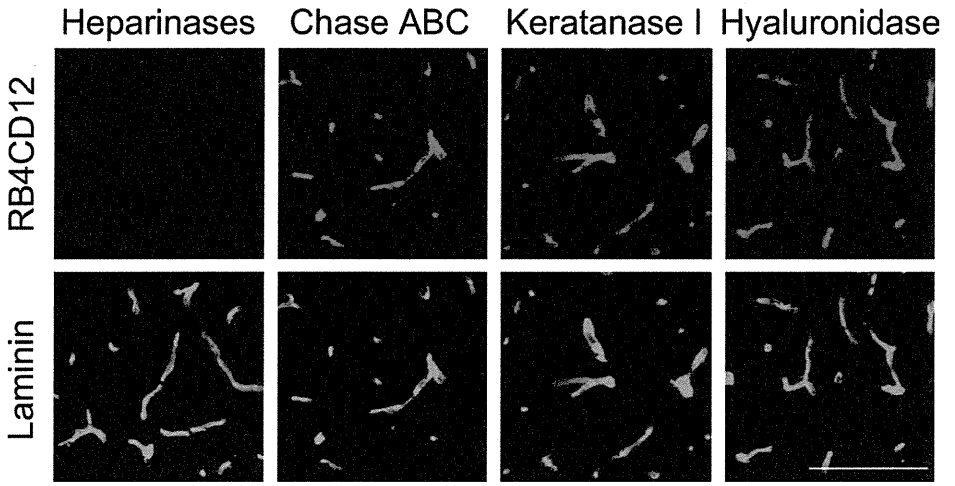

Fig. 3. Immunoreactivity of RB4CD12 is eliminated by pretreatment of brain sections with heparinases. Cryostat-cut sections of mouse brains were preincubated overnight with glyosaminoglycan-degrading enzymes. RB4CD12 binding was visualized using a Cy3-conjugated anti-VSV tag antibody with fluorescence microscopy (red). Basement membranes of vessels were costained using an antilaminin antibody in conjunction with a Cy2-conjugated secondary antibody (green). RB4CD12 signals in the microvasculature basement membrane of vessels were eliminated by a mixture of heparinase I, heparinase II, and heparinase III (Heparinases). Chase ABC, chondroitinase ABC. Scale bar = 50 μm.

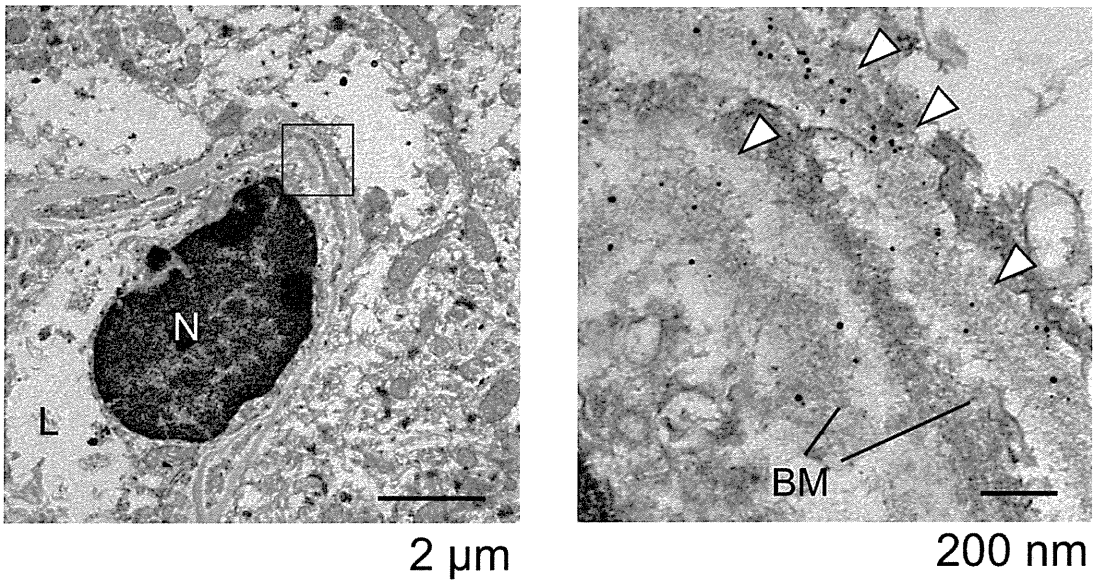

Fig. 4. Immunoelectron microscopy for the RB4CD12 epitope in the mouse brain. Low-magnification (**left**) and high-magnification (**right**) scanning electron micrographs. RB4CD12 immunogold particles, singly or in clusters, decorate electron-lucid layers in the basement membrane (BM) of a vessel indicated by arrowheads. N, nucleus; L, vessel lumen.

tions (Fig. 1A), suggesting that the RB4CD12 antibody is highly specific to a trisulfated disaccharide-containing HS oligosaccharide. *N*-desulfated heparin, chondroitin, and chondroitin 6-sulfate (CS-C) did not affect the RB4CD12 recognition. Pretreatment of the heparin-BSA with a mixture of heparitinases eliminated the RB4CD12 recognition (Fig. 1B).

The RB4CD12 Epitope Is Abundant in the Basement Membrane of Vessels in the Brain

Previous study has shown that different HS epitopes should have a defined distribution and be tightly topologically regulated (Dennissen et al., 2002). To determine whether expression of the trisulfated disaccharide-containing HS is spatially regulated in the brain, we

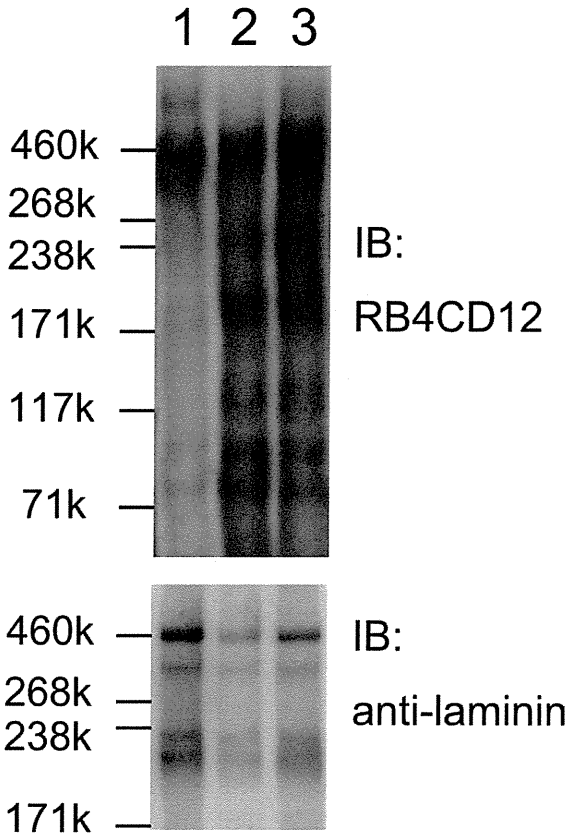

Fig. 5. Immunoblotting analysis of the RB4CD12 epitope in vessel-enriched fractions of the mouse cortex. Immunoblot with RB4CD12 and antilaminin antibodies for vessel-enriched fractions of the mouse cortex. Lane 1, vessel-enriched fraction; lane 2, flow-through fraction; lane 3, whole-cortex fraction.

immunohistochemically analyzed the distribution of the RB4CD12 epitope in the brain. Cryostat-cut sections of C57BL/6 mouse brains were immunostained with the RB4CD12 antibody and each cell type-specific antibody. As shown in Figure 2, RB4CD12 staining signals clearly colocalized with laminin, which is abundant in the basement membrane of vessels and is used as a marker for brain vasculature (Laurie et al., 1982). GFAP, a marker for astrocytes, partially colocalized with the RB4CD12 staining signals at the gliovascular interface (Fig. 2, arrowheads). The RB4CD12 epitope was hardly detected in cells that were positive for NeuN, a marker for neurons. Neither IbaI, a marker for microglia, nor CNPase, a marker for oligodendrocytes, was immunolocalized with the RB4CD12 staining signals (Fig. 2). WFA lectin, which is often used as a marker for perineuronal nets that are rich in chondroitin sulfates, did not colocalize with the RB4CD12 signals (Fig. 2). Similar results were also observed in the hippocampus and cerebellum (not shown). These results indicated that the RB4CD12 epitope exists in large quantities in the basement membrane of brain vessels. To confirm that the observed signals in Figure 2 arose from a trisulfated disaccharide-containing HS oligosaccharide, we pretreated brain sections with a mixture of heparinases, chondroitinase ABC, karatanase I, or hyaluronidase and then stained with the RB4CD12 antibody and an antilaminin antibody. Only treatment with a mixture of heparinases eliminated RB4CD12 immunoreactivity (Fig. 3). To determine the ultrastructural localization of the RB4CD12 epitope in the basement membrane of the brain vessels, we carried out immunoelectron microscopy. Cryostat-cut sections from C57BL/6 mouse brains were immunostained with the RB4CD12 antibody followed by probing with a rabbit anti-VSV secondary antibody and a goat anti-rabbit IgG tertiary antibody conjugated with gold particles. After enlargement of the gold particles, the specimens were embedded in water-miscible epoxy resins and examined under a transmission electron microscope. We observed that most RB4CD12 immunogold particles were present in the area of the basement membrane of cerebral vessels (Fig. 4, right panel, arrowheads).

The RB4CD12 Epitope Is Borne Predominantly on Molecules of 460 kDa in Vessel-Enriched Fractions

Next, we prepared vessel-enriched fractions of mouse cortices and examined the immunoreactivity of the RB4CD12 antibody. Immunoblotting with the antilaminin antibody indicated that the vessel-enriched fraction was properly fractionated (Fig. 5, lower panel). A band with a molecular weight of ~460 kDa was dominant in an immunoblot with the RB4CD12 antibody in the vessel-enriched fractions (Fig. 5).

Trisulfated Disaccharides of Heparan Sulfate Are Detected in Vessel-Enriched Fractions

Finally, we carried out structural analysis of HS chains in the vessel-enriched fractions of mouse brain. HS was isolated from the whole cortex and the cortical vessel-enriched fractions of adult mice and depolymerized into its constituent disaccharides by a mixture of bacterial heparitinases. The disaccharide compositions of the HS were determined by reversed-phase ion-pair chromatography. We found that 2.3% of the total disaccharides were trisulfated disaccharides in the vessel-enriched fractions. The presence of the trisulfated disaccharides was consistent with the fact that RB4CD12 recognizes the vessels in the brain. The content of total HS in the vessel-enriched fractions of the adult mouse cortex was 5% of that in the whole-cortex fraction (Fig. 6).

DISCUSSION

The present study shows that the immunoreactivity of the RB4CD12 antibody was colocalized with the laminin immunoreactivity, suggesting that the RB4CD12 epitope is present largely in the basement membrane of vessels in the brain. The immunoelectron microscopic analysis confirmed the localization of the

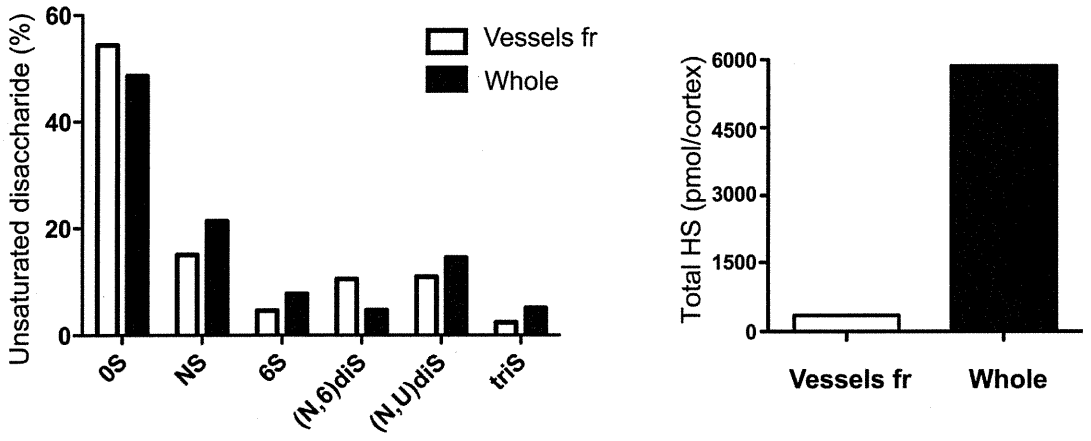

	Disaccharide composition (% of total disaccharides)						Total HS (pmol/cortex)
	0S	NS	6S	(N,6)diS	(N,U) diS	triS	HS
vessels fr	55.0	16.9	4.3	10.7	10.7	2.3	286.8
whole	48.4	20.5	7.0	4.4	14.7	5.0	5616.0

Fig. 6. Disaccharide analysis of heparan sulfate in vessel-enriched fractions of the mouse cortex. Heparan sulfates were purified from whole tissues (whole) or vessel-enriched fractions (vessels fr) of mouse cerebral cortices and then degraded with a mixture of heparinases I, II, and III. The produced disaccharides were analyzed by postlabeling reversed-phase ion-pair HPLC. The values are representative of two independent experiments.

RB4CD12 epitope in the vascular basement membrane. These findings are correlated with those of a previous report that demonstrated that RB4CD12 stains the skeletal muscle basal lamina (Jenniskens et al., 2000). We also found that the RB4CD12-positive ~460-kDa band was present in the immunoblot of the vessel-enriched fractions. Perlecan, agrin, and type XVIII collagen are the major HSPGs present in the basement membrane of the brain vasculature (Bezakova and Ruegg, 2003; Iozzo, 2005). The size of the core protein of perlecan is known to be ~460 kDa. It can reach a molecular weight of over 800 kDa together with HS chains. Agrin has a 225-kDa core protein, and its glycosylation modifications increase the molecular weight to ~500 kDa in the brain (Donahue et al., 1999). Type XVIII collagen shows molecular weights of ~200 kDa (Elamaa et al., 2003). Our results from Western blotting suggest that the observed immunoreactivity of the RB4CD12 antibody in the cortex might arise from the HS chains of perlecan and/or agrin. Further investigation is needed for identification of the core proteins that bear the RB4CD12 epitope expressed in the brain vasculature.

In conjunction with the RB4CD12 immunoreactivity in the laminin-positive basement membrane and vessel-enriched fractions, the disaccharide analysis showed that trisulfated disaccharides are components of HS chains in the vessel-enriched fractions. Although the percentage of trisulfated disaccharides is not substantial, it is possible that these disaccharides are clustered and form highly sulfated domains that are RB4CD12 recognition determinants within the chains. The recognition epitope of RB4CD12 is proposed to be [–GlcNSO$_3$(6-OSO$_3$)-IdoA(2-OSO$_3$)-GlcNSO$_3$(6-OSO$_3$)–] (Jenniskens et al., 2002), so the cluster size might be two or more consecutive trisulfated disaccharides. It is known that *N*-sulfation of GlcN residues is the initial HS sulfation and that *N*-sulfated domains are primary sites for further modification (Carlsson et al., 2008). It seems probable that *N*-sulfation could occur densely, not sparsely, in the brain vasculature, leading to the formation of trisulfated disaccharide clusters within HS polysaccharides. Expression profiles of HS sulfotransferases and sulfatases in brain vessels may provide approaches that are pertinent to understanding the mechanisms underlying the formation of the HS subdomains.

Sulf-1 and Sulf-2 are known to remove 6-*O* sulfates on glucosamine residues in the trisulfated disaccharides of HS and heparin (Morimoto-Tomita et al., 2002; Ai et al., 2003; Viviano et al., 2004; Saad et al., 2005). Sulf-2 mobilizes heparin-bound vascular endothelial growth factor (VEGF), fibroblast growth factor (FGF)-1, and stromal cell-derived factor (SDF)-1/CXCL12 (Uchimura et al., 2006). Our previous study has shown that treatment of mouse brain sections with Sulf-1 or Sulf-2 diminished the immunoreactivity of RB4CD12 in the brain vessels ex vivo (Hossain et al., 2010). Given the results of the present study, the RB4CD12-positive HS subdomains might be important for supporting interactions between HS chains and macromolecules such as growth factors in the basement membrane of the brain vessels. Increasing evidence has shown that highly sulfated domains within HS chains of HSPGs support the interaction with HS-binding factors. VEGF binds to perlecan (Jiang and Couchman, 2003). HSPGs could act

as storage sites of VEGF in the vessel wall. The release of growth factors from the complex with HSPGs through proteolytic processing and HS degradation is a physiological mechanism that disengages biologically active molecules from its storage site (Iozzo, 1998; Bergers et al., 2000). In the basement membrane of vessels, VEGF is stored by binding to HSPGs and could be released by the action of Sulfs to exert proangiogenic activity (Morimoto-Tomita et al., 2005; Uchimura et al., 2006). Our results describing the abundance of the RB4CD12 epitope in the basement membrane of the brain vessels could emphasize the roles of the trisulfated disaccharide-containing HS domains in the storage and release of HS-bound growth factors, especially VEGF. Furthermore, endothelial cells bind to the perlecan protein core (Hayashi et al., 1992), which is modulated by the presence of glycosaminoglycan chains. Our results also highlight a possible role of the RB4CD12 epitope in migration and growth of endothelial cells in the brain vasculature. Within an angiogenic niche, adult neurogenesis has been shown to occur (Palmer et al., 2000). Growth factors that are bound to the RB4CD12-positive HS subdomains might be involved in defining the neurogenic microenvironment. Future efforts to investigate the biological roles of the RB4CD12 epitope and the Sulfs in brain vessels will provide essential information on the contribution of the trisulfated disaccharide-containing HS domains to cerebrovascular angiogenesis and neurogenesis.

ACKNOWLEDGMENTS

We thank Steven Rosen and Tony Wyss-Coray for their helpful suggestions and discussion. We are grateful to Kuniko Takanose for technical assistance. T.H.-F. is a Research Fellow of the Japan Foundation for Aging and Health.

REFERENCES

Ai X, Do AT, Lozynska O, Kusche-Gullberg M, Lindahl U, Emerson CP Jr. 2003. QSulf1 remodels the 6-*O* sulfation states of cell surface heparan sulfate proteoglycans to promote Wnt signaling. J Cell Biol 162:341–351.

Bergers G, Brekken R, McMahon G, Vu TH, Itoh T, Tamaki K, Tanzawa K, Thorpe P, Itohara S, Werb Z, Hanahan D. 2000. Matrix metalloproteinase-9 triggers the angiogenic switch during carcinogenesis. Nat Cell Biol 2:737–744.

Bernfield M, Gotte M, Park PW, Reizes O, Fitzgerald ML, Lincecum J, Zako M. 1999. Functions of cell surface heparan sulfate proteoglycans. Annu Rev Biochem 68:729–777.

Bezakova G, Ruegg MA. 2003. New insights into the roles of agrin. Nat Rev Mol Cell Biol 4:295–308.

Bishop JR, Schuksz M, Esko JD. 2007. Heparan sulphate proteoglycans fine-tune mammalian physiology. Nature 446:1030–1037.

Carlsson P, Presto J, Spillmann D, Lindahl U, Kjellen L. 2008. Heparin/heparan sulfate biosynthesis: processive formation of *N*-sulfated domains. J Biol Chem 283:20008–20014.

Dennissen MA, Jenniskens GJ, Pieffers M, Versteeg EM, Petitou M, Veerkamp JH, van Kuppevelt TH. 2002. Large, tissue-regulated domain diversity of heparan sulfates demonstrated by phage display antibodies. J Biol Chem 277:10982–10986.

Donahue JE, Berzin TM, Rafii MS, Glass DJ, Yancopoulos GD, Fallon JR, Stopa EG. 1999. Agrin in Alzheimer's disease: altered solubility and abnormal distribution within microvasculature and brain parenchyma. Proc Natl Acad Sci U S A 96:6468–6472.

Elamaa H, Snellman A, Rehn M, Autio-Harmainen H, Pihlajaniemi T. 2003. Characterization of the human type XVIII collagen gene and proteolytic processing and tissue location of the variant containing a frizzled motif. Matrix Biol 22:427–442.

Esko JD, Lindahl U. 2001. Molecular diversity of heparan sulfate. J Clin Invest 108:169–173.

Esko JD, Selleck SB. 2002. Order out of chaos: assembly of ligand binding sites in heparan sulfate. Annu Rev Biochem 71:435–471.

Gallagher JT. 2001. Heparan sulfate: growth control with a restricted sequence menu. J Clin Invest 108:357–361.

Habuchi H, Habuchi O, Kimata K. 2004. Sulfation pattern in glycosaminoglycan: does it have a code? Glycoconj J 21:47–52.

Habuchi H, Nagai N, Sugaya N, Atsumi F, Stevens RL, Kimata K. 2007. Mice deficient in heparan sulfate 6-*O*-sulfotransferase-1 exhibit defective heparan sulfate biosynthesis, abnormal placentation, and late embryonic lethality. J Biol Chem 282:15578–15588.

Hayashi K, Madri JA, Yurchenco PD. 1992. Endothelial cells interact with the core protein of basement membrane perlecan through beta 1 and beta 3 integrins: an adhesion modulated by glycosaminoglycan. J Cell Biol 119:945–959.

Hossain MM, Hosono-Fukao T, Tang R, Sugaya N, van Kuppevelt TH, Jenniskens GJ, Kimata K, Rosen SD, Uchimura K. 2010. Direct detection of HSulf-1 and HSulf-2 activities on extracellular heparan sulfate and their inhibition by PI-88. Glycobiology 20:175–186.

Iozzo RV. 1998. Matrix proteoglycans: from molecular design to cellular function. Annu Rev Biochem 67:609–652.

Iozzo RV. 2005. Basement membrane proteoglycans: from cellar to ceiling. Nat Rev Mol Cell Biol 6:646–656.

Jenniskens GJ, Oosterhof A, Brandwijk R, Veerkamp JH, van Kuppevelt TH. 2000. Heparan sulfate heterogeneity in skeletal muscle basal lamina: demonstration by phage display-derived antibodies. J Neurosci 20:4099–4111.

Jenniskens GJ, Hafmans T, Veerkamp JH, van Kuppevelt TH. 2002. Spatiotemporal distribution of heparan sulfate epitopes during myogenesis and synaptogenesis: a study in developing mouse intercostal muscle. Dev Dyn 225:70–79.

Jiang X, Couchman JR. 2003. Perlecan and tumor angiogenesis. J Histochem Cytochem 51:1393–1410.

Lamanna WC, Frese MA, Balleininger M, Dierks T. 2008. Sulf loss influences *N*-, 2-*O*-, and 6-*O*-sulfation of multiple heparan sulfate proteoglycans and modulates fibroblast growth factor signaling. J Biol Chem 283:27724–27735.

Laurie GW, Leblond CP, Martin GR. 1982. Localization of type IV collagen, laminin, heparan sulfate proteoglycan, and fibronectin to the basal lamina of basement membranes. J Cell Biol 95:340–344.

Lemjabbar-Alaoui H, van Zante A, Singer MS, Xue Q, Wang YQ, Tsay D, He B, Jablons DM, Rosen SD. 2010. Sulf-2, a heparan sulfate endosulfatase, promotes human lung carcinogenesis. Oncogene 29:635–646.

Morimoto-Tomita M, Uchimura K, Werb Z, Hemmerich S, Rosen SD. 2002. Cloning and characterization of two extracellular heparin-degrading endosulfatases in mice and humans. J Biol Chem 277:49175–49185.

Morimoto-Tomita M, Uchimura K, Bistrup A, Lum DH, Egeblad M, Boudreau N, Werb Z, Rosen SD. 2005. Sulf-2, a proangiogenic heparan sulfate endosulfatase, is upregulated in breast cancer. Neoplasia 7:1001–1010.

Nakato H, Kimata K. 2002. Heparan sulfate fine structure and specificity of proteoglycan functions. Biochim Biophys Acta 1573:312–318.

Palmer TD, Willhoite AR, Gage FH. 2000. Vascular niche for adult hippocampal neurogenesis. J Comp Neurol 425:479–494.

Parish CR. 2006. The role of heparan sulphate in inflammation. Nat Rev 6:633–643.

Risau W, Wolburg H. 1990. Development of the blood–brain barrier. Trends Neurosci 13:174–178.

Saad OM, Ebel H, Uchimura K, Rosen SD, Bertozzi CR, Leary JA. 2005. Compositional profiling of heparin/heparan sulfate using mass spectrometry: assay for specificity of a novel extracellular human endosulfatase. Glycobiology 15:818–826.

Toyoda H, Kinoshita-Toyoda A, Selleck SB. 2000. Structural analysis of glycosaminoglycans in *Drosophila* and *Caenorhabditis elegans* and demonstration that *tout-velu*, a *Drosophila* gene related to EXT tumor suppressors, affects heparan sulfate in vivo. J Biol Chem 275:2269–2275.

Uchimura K, Morimoto-Tomita M, Bistrup A, Li J, Lyon M, Gallagher J, Werb Z, Rosen SD. 2006. HSulf-2, an extracellular endoglucosamine-6-sulfatase, selectively mobilizes heparin-bound growth factors and chemokines: effects on VEGF, FGF-1, and SDF-1. BMC Biochem 7:2.

Uchimura K, Lemjabbar-Alaoui H, van Kuppevelt TH, Rosen SD. 2010. Use of a phage display antibody to measure the enzymatic activity of the Sulfs. Methods Enzymol 480:51–64.

van den Born J, Salmivirta K, Henttinen T, Ostman N, Ishimaru T, Miyaura S, Yoshida K, Salmivirta M. 2005. Novel heparan sulfate structures revealed by monoclonal antibodies. J Biol Chem 280:20516–20523.

van Kuppevelt TH, Dennissen MA, van Venrooij WJ, Hoet RM, Veerkamp JH. 1998. Generation and application of type-specific anti-heparan sulfate antibodies using phage display technology. Further evidence for heparan sulfate heterogeneity in the kidney. J Biol Chem 273:12960–12966.

Viviano BL, Paine-Saunders S, Gasiunas N, Gallagher J, Saunders S. 2004. Domain-specific modification of heparan sulfate by Qsulf1 modulates the binding of the bone morphogenetic protein antagonist Noggin. J Biol Chem 279:5604–5611.

Yan D, Lin X. 2009. Shaping morphogen gradients by proteoglycans. Cold Spring Harbor Perspect Biol 1:a002493.

THE JOURNAL OF BIOLOGICAL CHEMISTRY VOL. 286, NO. 8, pp. 6393–6401, February 25, 2011

Lipoprotein Lipase Is a Novel Amyloid β (Aβ)-binding Protein That Promotes Glycosaminoglycan-dependent Cellular Uptake of Aβ in Astrocytes*[S]

Received for publication, August 4, 2010, and in revised form, November 23, 2010 Published, JBC Papers in Press, December 21, 2010, DOI 10.1074/jbc.M110.172106

Kazuchika Nishitsuji[‡], Takashi Hosono[‡], Kenji Uchimura[‡§], and Makoto Michikawa[‡1]

From the [§]Section of Pathophysiology and Neurobiology, [‡]Department of Alzheimer's Disease Research, National Center for Geriatrics and Gerontology, Obu, Aichi 474-8511, Japan

Lipoprotein lipase (LPL) is a member of a lipase family known to hydrolyze triglyceride molecules in plasma lipoprotein particles. LPL also plays a role in the binding of lipoprotein particles to cell-surface molecules, including sulfated glycosaminoglycans (GAGs). LPL is predominantly expressed in adipose and muscle but is also highly expressed in the brain where its specific roles are unknown. It has been shown that LPL is colocalized with senile plaques in Alzheimer disease (AD) brains, and its mutations are associated with the severity of AD pathophysiological features. In this study, we identified a novel function of LPL; that is, LPL binds to amyloid β protein (Aβ) and promotes cell-surface association and uptake of Aβ in mouse primary astrocytes. The internalized Aβ was degraded within 12 h, mainly in a lysosomal pathway. We also found that sulfated GAGs were involved in the LPL-mediated cellular uptake of Aβ. Apolipoprotein E was dispensable in the LPL-mediated uptake of Aβ. Our findings indicate that LPL is a novel Aβ-binding protein promoting cellular uptake and subsequent degradation of Aβ.

Lipoprotein lipase (LPL)[2] catalyzes the hydrolysis of triacylglycerol and mediates the cellular uptake of lipoproteins by functioning as a "bridging molecule" between lipoproteins and sulfated glycosaminoglycans (GAGs) or lipoprotein receptors in blood vessels (1, 2). Sulfated GAGs are side chains of proteoglycans normally found in the extracellular matrix and on the cell surface in the peripheral tissues and brain. Sulfation modifications vary within the GAG chains and are crucial for interaction between GAGs and various protein ligands (3), including LPL (4, 5).

It has been shown that LPL is distributed in numerous organs and is highly expressed in the brain (6, 7). Although the catabolic activity of LPL on triacylglycerol is observed in the brain (8), the finding that apolipoprotein CII (apoCII), an essential cofactor for LPL, is not expressed in the brain (9, 10), suggests that LPL has a novel nonenzymatic function in the brain. However, little is known about LPL function in the brain. Interestingly, it has been shown that LPL is accumulated in senile plaques of Alzheimer disease (AD) brains (11). Moreover, SNPs in the coding region of the LPL gene are associated with disease incidence in clinically diagnosed AD subjects, LPL mRNA expression level, brain cholesterol level, and the severity of AD pathologies, including neurofibrillary tangles and senile plaque density (12). These results suggest that LPL may have a physiological role in the brain, whose alternation is associated with the pathogenesis of AD.

The occurrence of senile plaques in the brain is one of the pathological hallmarks of AD. They contain extracellular deposits of amyloid β protein (Aβ), and the abnormal Aβ deposition or the formation of soluble Aβ oligomers is crucial for AD pathogenesis. Aβ is a physiological peptide whose main species are 40 and 42 amino acids in length, and Aβ42 is the predominant specie in senile plaques (13). The Aβ levels are determined by the balance between its production and degradation/clearance, and an attenuated Aβ catabolism is suggested to cause Aβ accumulation in aging brains (14). Previous studies have shown that astrocytes and microglia directly take up and degrade Aβ42 (15, 16) and that Aβ degradation occurs in late endosomal-lysosomal compartments (17, 18). These lines of evidence, together with the finding that LPL mediates the cellular uptake of lipoproteins (1, 2), led us to carry out experiments to determine whether LPL interacts with Aβ to promote Aβ cellular uptake and degradation in astrocytes. Here, we provide evidence that LPL forms a complex with Aβ and facilitates Aβ cell surface binding and uptake in mouse primary astrocytes through a mechanism that is dependent on heparan sulfate and chondroitin sulfate GAG chains, leading to the lysosomal degradation of Aβ.

MATERIALS AND METHODS

Materials—Bovine LPL, heparinases, and a polyclonal anti-actin antibody were purchased from Sigma. Synthetic Aβ1–42 was purchased from the Peptide Institute (Osaka,

* This work was supported by a grant-in-aid for scientific research on priority areas (Research on Pathomechanisms of Brain Disorders) from the Ministry of Education, Culture, Sports, Science, and Technology of Japan, a grant from the Program for Promotion of Fundamental Studies in Health Sciences of the National Institute of Biomedical Innovation, a grant from the Ministry of Health, Labor, and Welfare of Japan (Research on Dementia, Health, and Labor Sciences Research Grant H20-007), and a grant from the Japan Health Sciences Foundation (Research on Publicly Essential Drugs and Medical Devices).

[S] The on-line version of this article (available at http://www.jbc.org) contains supplemental "Methods" and Fig. 1.

[1] To whom correspondence should be addressed: Department of Alzheimer's Disease Research, National Center for Geriatrics and Gerontology, Gengo 35, Morioka, Obu, Aichi 474-8511, Japan. Tel.: 81-562-46-2311; Fax: 81-562-46-8569; E-mail: michi@ncgg.go.jp.

[2] The abbreviations used are: LPL, lipoprotein lipase; Aβ, amyloid β; ApoE, apolipoprotein E; CS, chondroitin sulfate(s); HS, heparan sulfate; GAG, glycosaminoglycan; ANOVA, one-way analysis of variance.

Japan). Heparin, chondroitin, chondroitin sulfates, and chondroitinase ABC were from Seikagaku (Tokyo, Japan). Monoclonal anti-Aβ antibodies (6E10, 4G8) were purchased from Signet Laboratories (Dedham, MA), and a goat polyclonal anti-ApoE antibody and mouse control IgG were from Millipore (Bedford, MA). An anti-LPL antibody and Cy3- and FITC- conjugated secondary antibodies were purchased from Abcam, Inc. (Cambridge, MA). A monoclonal anti-Aβ antibody (2C8) was purchased from Medical and Biological Laboratories (Nagoya, Japan).

Animals—C57BL/6 mice were purchased from SLC, Inc. (Hamamatsu, Japan). ApoE-KO mice were obtained from Jackson ImmunoResearch Laboratories (Bar Harbor, ME). The National Center of Geriatrics and Gerontology Institutional Animal Care and Use Committee approved the animal studies.

Preparation of LPL—Because the sequence of LPL is highly conserved among mammalian species and the ability of LPL to interact with proteoglycans is also well conserved, we used LPL purified from bovine milk. An LPL suspension (suspended in 3.8 M ammonium sulfate, 0.02 M Tris-HCl, pH 8.0) was centrifuged (10,000 × *g* for 20 min at 4 °C), and the resulting pellet was dissolved in PBS. The prepared LPL was stored at 4 °C and used within 3 days.

Cell Culture—Highly astrocyte-rich cultures were prepared according to a method described previously (19). In brief, brains of postnatal day 2 C57BL/6 mice or ApoE knock-out mice were removed under anesthesia. The cerebral cortices from the mouse brains were dissected, freed from meninges, and diced into small pieces; the cortical fragments were incubated in 0.25% trypsin and 20 mg/ml DNase I in PBS at 37 °C for 20 min. The fragments were then dissociated into single cells by pipetting. The dissociated cells were seeded in 75-cm^2 dishes at a density of 5×10^7 cells per flask in DMEM-containing 10% FBS. After 10 days of incubation *in vitro*, flasks were shaken at 37 °C overnight, and the remaining astrocytes in the monolayer were trypsinized (0.1%) and reseeded. The astrocyte-rich cultures were maintained in DMEM-containing 10% FBS until use.

Assay of Aβ Binding and Uptake in Astrocytes by Western Blotting—Assays were carried out on confluent monolayers of astrocytes grown in 12-well plates. Aβ was dissolved in dimethyl sulfoxide to a final concentration of 1 mM and stored at −40 °C. Aβ (500 nM) and LPL (1–10 μg/ml) were mixed in DMEM. Immediately, the mixture was added to the culture medium of astrocytes. Cells were incubated at 37 °C for 5 h to assess the cellular uptake of Aβ or at 4 °C for 3 h to evaluate the binding of Aβ to the cell surface of astrocytes. In these assays, cells were incubated in serum-free DMEM. After incubation, cells were washed with PBS three times, harvested using a cell scraper and lysed by sonication in radioimmune precipitation assay buffer (1% Nonidet P-40, 0.5% sodium deoxycholate, 0.1% SDS, 150 mM NaCl, 50 mM Tris-HCl (pH 8.0), 1 mM EDTA). Cell lysates were subjected to SDS-PAGE with 4–20% gradient gels (WAKO Pure Chemicals, Osaka, Japan) and transferred to polyvinylidene difluoride membranes (Millipore). Aβ was probed with 6E10 antibody followed by horseradish peroxidase-labeled anti-mouse antibody (Cell Signaling Technology, Inc., Beverly, MA) and chemiluminescent substrate ECL Plus (GE Healthcare). The protein contents of cell lysates were normalized to the expression level of actin protein. To examine the involvement of GAGs, heparin, chemically modified heparins, chondroitin, or chondroitin sulfates (3 μg/ml) were incubated with a mixture solution of Aβ and LPL. Astrocytes were pretreated with a mixture of heparinase II and heparinase III or chondroitinase ABC (0.03 units/ml) for 24 h at 37 °C to evaluate endogenously expressed glycosaminoglycans. Signals were visualized and quantified using a LAS-3000 luminescent image analyzer (Fujifilm, Tokyo, Japan) and ImageJ software (National Institutes of Health, Bethesda, MD). For analyzing protein band densities, a region of interest was drawn around a band, and protein band densities were calculated.

siRNA Interference of LPL—siRNA specific for mouse LPL (sense strand, 5′-CAGCUGAGGACACUUGUCAUCU-CAUdTdT-3′; antisense strand, 5′-AUGAGAUGACAAGU-GUCCUCAGCUGdTdT-3′) and control siRNA (sense strand, 5′-CAGAGGGCACAUUUGACCUUUCCAUdTdT-3′; antisense strand, 5′-AUGGAAAGGUCAAAUGUGCCCUCUG-3′) was purchased from Invitrogen. Astrocytes grown in 12-well plates for 24 h were transfected with either LPL siRNA or control siRNA with Lipofectamine RNAiMAX (Invitrogen). Forty-eight hours after transfection, cells were treated with Aβ (1 μM) and then incubated at 4 °C for 3 h, and cell-surface associated Aβ was analyzed as described above. An anti-LPL antibody (Gene Tex, Inc.) was used for the detection of LPL.

Assay of Aβ Degradation in Astrocytes—Astrocytes were incubated with Aβ (250 nM) and LPL (2 μg/ml) at 37 °C for 5 h. Subsequently, cells were washed with DMEM and incubated in DMEM for additional hours. Then, Aβ in cell lysates was analyzed by Western blotting as described above.

Immunoprecipitation—Aβ (500 nM) and LPL at various concentrations were incubated in DMEM at 37 °C for 3 h. LPL-Aβ complexes were immunoprecipitated with an anti-LPL antibody and magnetic protein G beads (Dynal, Hamburg, Germany). For detection of LPL-Aβ complexes in the mice brains, brain homogenates from 12-week-old C57BL/6 mice were used. In brief, anesthetized mice were perfused with PBS containing 35 μg/ml heparin for 15 min. The cerebrum was dissected out and homogenized by sonication in 4 volumes of PBS containing a protease inhibitor mixture (P8340; Sigma) and centrifuged at 1,000 × *g* for 10 min at 4 °C. The supernatants were harvested and LPL-Aβ complexes were immunoprecipitated with an anti-LPL antibody and magnetic protein G beads. The obtained precipitates were washed three times with PBS and incubated at 70 °C for 10 min in SDS sample buffer. Dissociated Aβ recovered in the supernatant was assessed by Western blotting as described above. For detection of endogenous Aβ, the supernatants were subjected to SDS-PAGE with 4–20% gradient gels and transferred to polyvinylidene difluoride membranes. The membranes were exposed to microwave irradiation for 20 s, and Aβ was probed with 4G8 antibody followed by horseradish peroxidase-labeled anti-mouse antibody and the chemiluminescent substrate ECL Plus.